International Journal of Infrared and Millimeter Waves, Vol. 26, No. 2, February 2005 (© 2005)
DOI: 10.1007/s10762-005-3002-4

INVESTIGATION OF DIFFERENT INPUT-MATCHING MECHANISMS USED IN WIDE-BAND LNA DESIGN

Robert Hu[1] and Mark S. C. Yang[2]

[1]*Department of Electronics Engineering*
National Chiao Tung University, Hsin-Chu, Taiwan Republic of China
[2]*VIA Technologies, Taipei, Taiwan Republic of China*

Revised 9 December 2004

Abstract

This paper analyzes different input-matching mechanisms used in designing the wide-band amplifiers in general, and the low noise amplifiers (LNA) in particular, and their corresponding noise impact. Among them, the most promising one is the reactive-feedback circuit configuration, which is a combination of high-frequency inductive feedback and low frequency capacitive feedback. In this paper the simulated result that both matched input impedance and low noise temperature T_n can be achieved simultaneously over a wide bandwidth in the single-ended low noise amplifier is proved mathematically and is well interpreted. This understanding of reactive feedback is crucial for the future development of ultra-wide-band low-noise amplifiers.

Keywords: Input matching, wide-band, LNA, resistive feedback, inductive feedback, capacitive feedback, reactive feedback.

I. Introduction

High-quality wide-band LNA is in urgent demand in radio-astronomy community where the design emphasis has been on achieving both small input reflection coefficient and low noise temperature [1]-[4]. As is well known, the simplest way of achieving wide-band input matching is by adding either a shunt or a feedback resistor at the circuit s input stage; however, the incoming signal attenuation plus the resistor s thermal noise will make the resulting circuit very noisy. On the other hand, it is true that a transistor, when a source inductor and an input series inductor were connected to it, can have matched input impedance and optimized noise temperature locally. One might thus conclude that the only way making a wide-band LNA is either by using the balanced circuit configuration, which has twice the power dissipation, or by adding a bulky isolator in front of the amplifier.

However, there is one seemingly inductive-feedback LNA that does exhibit matched input impedance over wide bandwidth [5]. A rough guessing is attributing it to the finite isolation of the first-stage transistor and its complex output loading impedance; thus, by fine-tuning this loading impedance, the transistor's input impedance becomes quasi-constant over a broad bandwidth [6]. Elaborate circuit simulations further reveal that a transistor with an external source inductor and an *R-C* loading impedance does have wide-band matched input and flat noise temperature. As an extension of our previous LNA work [7], this paper will investigate several commonly-used wide-band matching mechanisms and details the newly-proposed reactive-feedback approach, all in terms of signal and noise respectively.

Section II starts with the small-signal and noise models of a high-electron-mobility transistor (HEMT). It is then followed by discussions on different wide-band resistive-feedback circuit configurations, with each has the noise impact of the added resistor clarified. Section III covers two narrowband lossless feedback mechanisms: the first is the inductive feedback intended for high-frequency input matching, and second is the capacitive feedback which has a matched input at low frequency. In additional to presenting the simulated results, both circuits' input impedance and noise temperature expressions will be derived and explained in depth. Only after the discussions on these two narrow-band mechanisms, the novel wide-band reactive feedback can be constructed and easily understood.

It needs to be emphasized that the design methodology for wide-band LNA is different from that of narrow-band one. In the narrow-band case, the targeted noise match is realized through some input tuning circuit [8]–[10]; in the wide-band case, since noise match occurs only at high end of the operating frequency range, the design goal is instead on how to reduce the minimum noise temperature and noise resistance so the extra mismatched noise can be reduced [11]. Furthermore, in this paper we do and need to take the effect of the intrinsic feedback capacitor C_{gd} into consideration in the circuit analysis; rather than treat it as a mere detrimental factor while omit it in the mathematical formulation, as most other authors do.

II. Review of Lossy Input-Matching Mechanisms

A. Transistor's small-signal and noise models

As the most critical component in the LNA, prior knowledge of both the transistor's small-signal model and noise models is necessary in designing the LNA circuits [12]–[15]. With the transistor operating at the maximum-gain bias

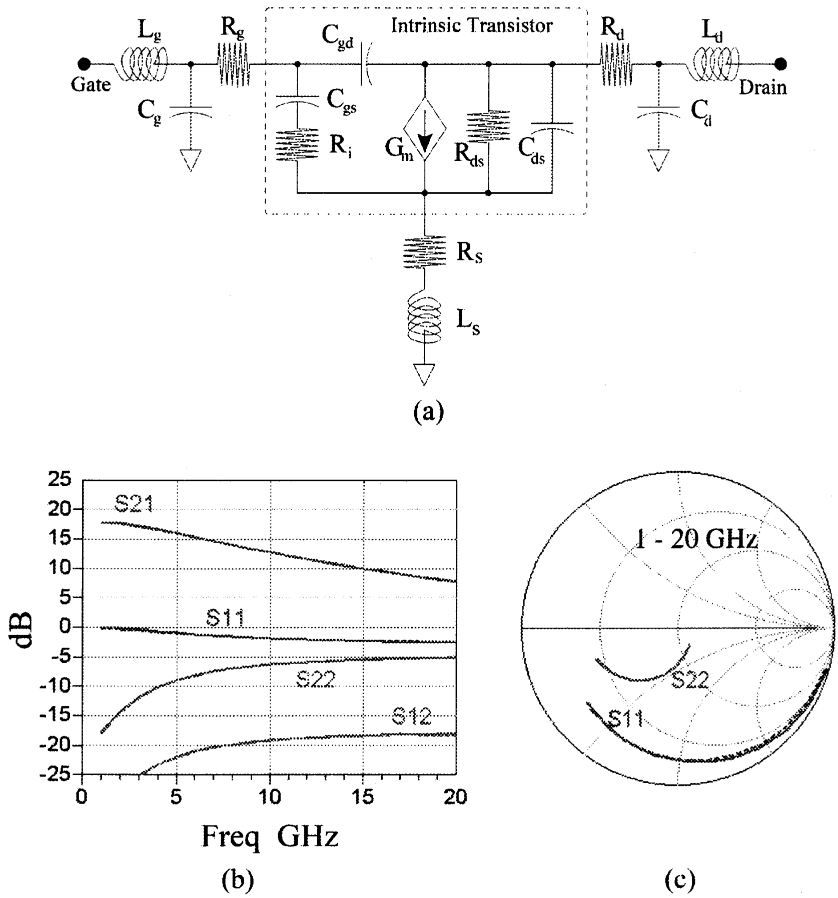

Fig. 1. Characteristics of the TRW 200-um HEMT. (a) The transistor's 15-element small-signal model with the intrinsic elements in the dotted box where the transconductance is $G_m \exp(j\omega\tau)$. When the transistor is biased at V_d = 0.6 V and I_d = 12 mA, there will be C_g = 8 fF, R_g = 3.4 Ω, L_g = 13 pH, C_d = 8 fF, R_d = 2.4 Ω, L_d = 14 pH, R_s = 0.8 Ω, L_s = 3 pH, C_{gs} = 115 fF, R_i = 0 Ω, C_{gd} = 59 fF, τ = 0 pSec, G_m = 175 mS, R_{ds} = 42 Ω, C_{ds} = 10 fF. (b) S-parameters in dB. (c) 1–20-GHz S_{11} and S_{22} on the Smith chart.

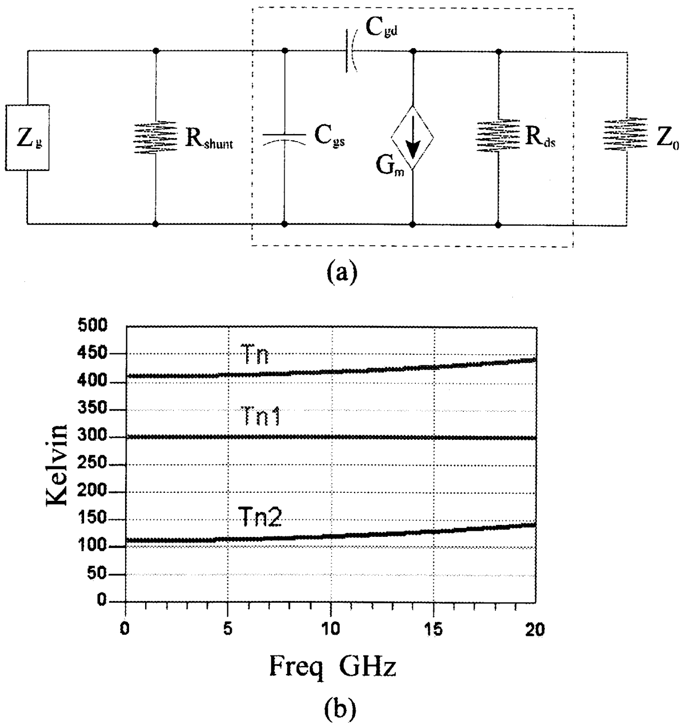

Fig. 2. Input matching using a shunt resistor. (a) Schematic. (b) Noise temperature of the transistor circuit with 50-Ω input shunt resistor R_{shunt}. T_{n1} is from R_{shunt} at 300 Kelvin, T_{n2} is from R_{ds} at 2100 Kelvin and T_n is the overall noise temperature, i.e. $T_n = T_{n1} + T_{n2}$.

point, its corresponding 15-element small-signal model can be easily derived (Fig. 1). The transistor's noise model is based on Pospieszalski's proposal where a temperature T_d is assigned to the transistor's drain resistor R_{ds} while temperature of all the other constituting components are set to ambient temperature T_{amb} [16]. The underlying assumption here is that there is no correlation in the intrinsic transistor's gate noise voltage vg and drain noise current i_d; therefore, vg can be assigned to gate resistor R_i and i_d to drain resistor R_{ds} with equivalent temperatures of T_{gate} and T_{drain} respectively. Empirically, T_g is close to T_{amb} while T_d needs to be very large, e.g. 2000–3000 Kelvin for a transistor at room temperature. Though, admittedly, this zero-correlation assumption is not impeccable [17], [18], it makes the following noise analysis much straightforward and thus more insightful. The formal noise-correlation matrix approach is reserved for device physics research and beyond the scope of this paper.

B. Wide-band input matching using a shunt resistor

While it seems quite a common sense placing a shunt resistor in front of the transistor to have a matched input over a wide bandwidth, signal loss at the input plus the thermal noise generated by the resistor itself lead to the inevitable deterioration of the circuit's noise performance (Fig. 2). Mathematically, when a shunt resistor R_{shunt} (= $1/G_{shunt}$) with temperature T_{amb} is connected to the transistor, the circuit's input admittance is

$$\begin{aligned} Y_{in} &= G_{shunt} + j\,\omega\,C_{in} \\ &= G_{shunt} + j\,\omega\,C_{gs} + j\,\omega\,C_{gd}\,\left[1 + G_m\,(R_{ds} \parallel Z_0)\right] . \end{aligned} \tag{1}$$

If G_{shunt} is far greater than ωC_{in}, then Y_{in} is close to G_{shunt} and the wide-band input matching can be achieved by setting G_{shunt} equal to the characteristic admittance Y_0.

As for noise, when a generator admittance Y_g (= $G_g + jB_g$) is presented at the input of the transistor circuit, this circuit's noise temperature can be split into the noise from the resistor, as T_{n1}, and the noise from the transistor itself, which is T_{n2}. This separation of noise temperature is made possible because of zero correlation between the two noise sources. By pairing the noise current of G_{shunt} to G_g, noise temperature T_{n1} can be obtained and is equal to $T_{amb}G_{shunt} = G_g$. Derivation of the more complicated T_{n2} expression can be greatly simplified by assuming a short-circuit output loading, as noise temperature is by definition independent of the output loading impedance. The overall noise temperature of the circuit is thus

$$\begin{aligned} T_n &= T_{amb}\,\frac{G_{shunt}}{G_g} \\ &\quad + \frac{T_{drain}}{G_m^2}\,\frac{1}{R_{ds}\,G_g}\,\left[(G_g + G_{shunt})^2 + (B_g + \omega\,C_{gs} + \omega\,C_{gd})^2\right] . \end{aligned} \tag{2}$$

Obviously, the smaller the shunt resistor is, the larger the resulting noise temperature will be.

C. Wide-band input matching using a feedback resistor

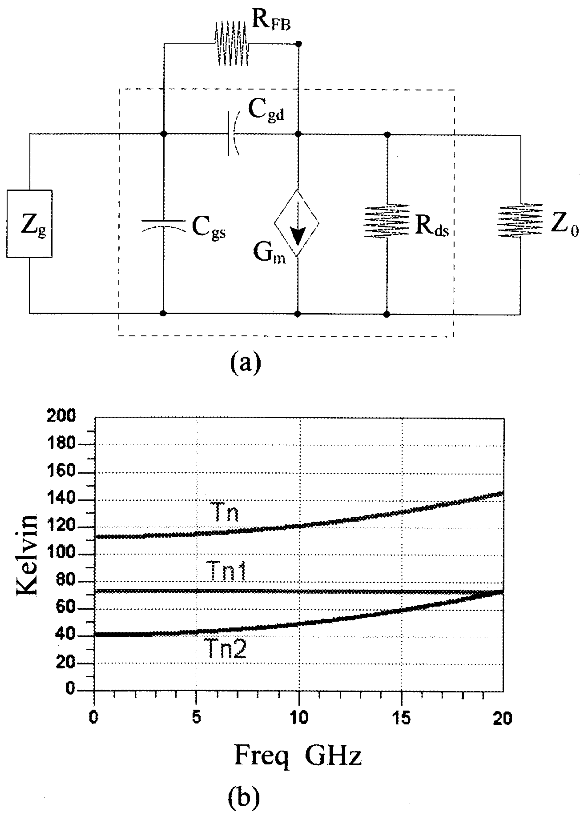

Fig. 3. Input matching using a feedback resistor. (a) Schematic. (b) Noise temperature of the transistor circuit with 270-Ω feedback resistor R_{FB}. Noise temperature T_{n1} is from R_{FB} at 300 Kelvin, T_{n2} is from R_{ds} at 2100 Kelvin and T_n is the overall noise temperature.

By connecting the transistor's gate and drain nodes using a resistor, a wide-band input matching can be achieved too [19]. Because a much larger resistor R_{FB} (= $1/G_{FB}$) is now used for lowering S_{11}, improved noise performance is expected when compared with the aforementioned hunt-resistor approach (Fig. 3). Mathematically, since both C_{gd} and R_{FB} branches are of high impedance for the induced current on the drain side, these two components can be transformed on the signal perspective into their equivalent input shunt counterparts:

$$\begin{aligned} C_{Miller} &= C_{gd}\, G_m\, [1 + (R_{ds} \parallel Z_0)] \\ G_{Miller} &= G_{FB}\, G_m\, [1 + (R_{ds} \parallel Z_0)]\,. \end{aligned} \tag{3}$$

For the TRW 200-um transistor, there is $[1 + (R_{ds} \| Z_0)] = 5.375$. Thus, instead of using a 50-Ω input shunt resistor for a matched input, a 268.75-Ω feedback resistor can be adopted to have the same effect.

Regarding the noise, the temperature T_{n2} due to the drain resistor R_{ds} at temperature T_{drain} has mathematical expression similar to that of the shunt-resistor case, i.e.

$$T_{n2} = \frac{T_{drain}}{G_m^2}\, \frac{1}{R_{ds}\, G_g}\, \left[(G_g + G_{FB})^2 + (B_g + \omega\, C_{gs} + \omega\, C_{gd})^2 \right]\,. \tag{4}$$

Noise temperature T_{n1} that comes from R_{FB} at temperature T_{amb} is

$$\begin{aligned} T_{n1} &= \frac{T_{amb}}{G_m^2}\, \frac{1}{R_{FB}\, G_g}\, \left[(G_g + 2\, G_{FB} + G_m)^2 + (B_g + \omega\, C_{gs} + \omega\, C_{gd})^2 \right] \\ &\equiv \frac{T_{amb}}{G_m^2}\, \frac{1}{R_{FB}\, G_g}\, \alpha\,. \end{aligned} \tag{5}$$

This T_{n1} expression looks similar to that of the transistor circuit with input shunt resistor except for the factor α. With 50-Ω generator impedance, 270-Ω R_{FB}, 175-mS G_m, and neglecting the small reactive part, α is 1.338 and T_{n1} will be 74 Kelvin for the transistor circuit at room temperature. In contrast, a shunt 50-Ω resistor used for achieving the same input reflection coefficient has T_{n1} close to 300 Kelvin.

III. Lossless Input-Matching Mechanisms: Inductive, Capacitive and Reactive Feedbacks

A. Narrow-band input matching using inductive feedback

Without resorting to the resistor, intended input matching can still be achieved, though narrow-band, by first adding an inductor L_{FB} on the transistor's source node (Fig. 4). Conceptually, the induced current I_L on the drain side will flow through this L_{FB} inductor and generate a voltage on it that is in phase with the input current. This L_{FB} can thus be interpreted as a resistor. Mathematically, based on the somehow simplified transistor model, there is

$$\begin{aligned} V_1 &= V_c + j\,\omega\, L_{FB}\, I_L \\ &= V_c + j\,\omega\, L_{FB}\, (j\,\omega\, C_{gs}\, V_c + G_m\, V_c) \\ &= \left(1 - \omega^2\, L_{FB}\, C_{gs} + j\,\omega\, L_{FB}\, G_m\right)\, V_c \\ &\approx (1 + j\,\omega\, L_{FB}\, G_m)\, V_c\,. \end{aligned} \tag{6}$$

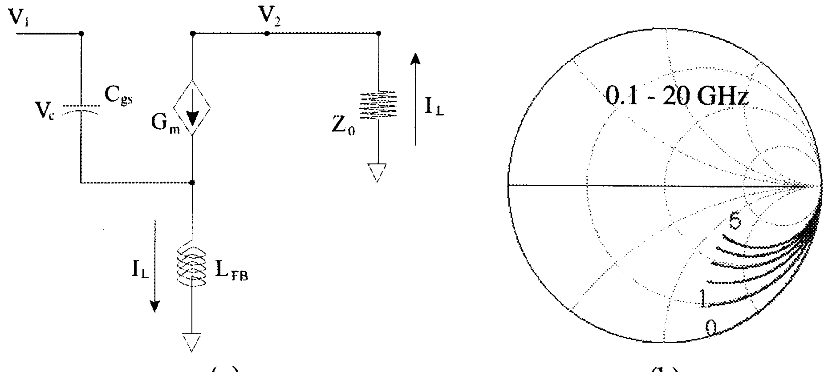

The last approximation holds because of the transistor's large G_m and small C_{gs}. For example, the TRW 200-um HEMT circuit with 50-Ω Re[Z_{in}] has, at 20 GHz,

Fig. 4. Inductive feedback using simplified transistor model. (a) In the schematic, the induced current I_L flowing through L_{FB} will bring upon a voltage on this inductor that is in phase with the input current. The current on the loading impedance Z_0 is assumed to be equal to that on L_{FB} because of the large impedance of C_{gs}. (b) 0.1–20-GHz S_{11} on the Smith chart. With C_{gs} = 113 fF, G_m = 175 mS, curves 0 to 5 correspond to L_{FB} = 0, 10, 20, 30, 40 and 50 pH respectively.

$$\omega^2 L_{FB} C_{gs} = \omega^2 \frac{C_{gs} Z_0}{G_m} C_{gs} = 0.057 \ll 1 . \tag{7}$$

In other words, the current flowing through C_{gs} will not contribute significantly to the voltage across L_{FB} and so the input impedance of this transistor circuit is a capacitor in series with a resistor:

$$Z_{in} = \frac{V_1}{(j\,\omega\, C_{gs})\, V_c} = \frac{1}{j\,\omega\, C_{gs}} + \frac{L_{FB}\, G_m}{C_{gs}} . \tag{8}$$

On the Smith chart, the inclusion of L_{FB} will split the transistor's S_{11} trajectory into different curves with each corresponding to different Re[Z_{in}]. To eliminate the remaining capacitive part of Z_{in}, an additional input series inductor L_{series} can then be added. As complete input matching now occurs only at one frequency, the inductive-feedback approach is deemed narrow-band.

Though, on the face of it, the above derivation looks trivial as it may have been worked out by other authors. The problem is that the transistor model used

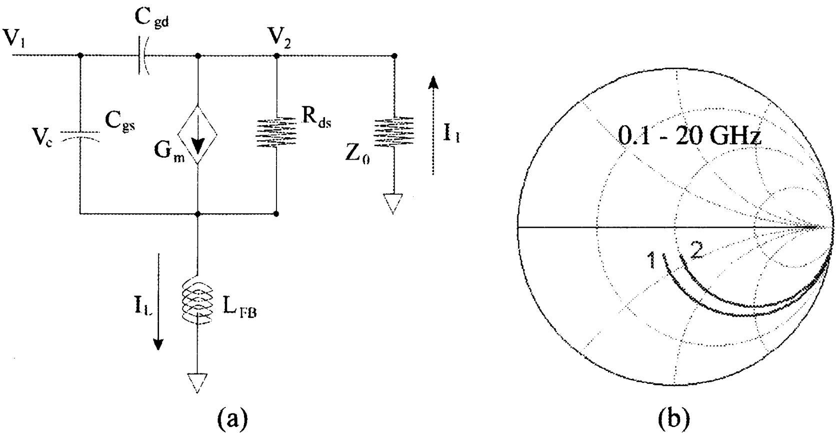

Fig. 5. Inductive feedback. (a) Once the 59-fF C_{gd} is added for better transistor modeling, the previously derived 30-pH L_{FB} turns to be too small for good input matching and needs to be increased.to 194 pH. When the 50-Ω R_{ds} is included, L_{FB} have to be changed to 250-pH again. Here the current on the loading impedance Z_0 is assumed to be the same as that on LFB because of the large impedance of C_{gs} and C_{gd}. (b) 0.1–20-GHz S_{11} on the Smith chart with curves 1 and 2 correspond to L_{FB} = 194 and 250 pH respectively.

above is over-simplified in the microwave frequency range; therefore, the calculated value of L_{FB} is far from accurate. With the intrinsic capacitor C_{gd} included, the new shunt impedance Z_{Miller} will appear in the Z_{in} expression. The revised derivation is presented in the following. First, the voltage across C_{gd} is

$$\begin{aligned} V_1 - V_2 &= (1 + j\,\omega\, L_{FB}\, G_m + G_m\, Z_0)\; V_c \\ &= \left[1 + \left(j\,\frac{\omega\, L_{FB}}{Z_0} + 1\right)\, G_m\, Z_0\right]\, V_c \\ &\approx (1 + G_m\, Z_0)\; V_c\,. \end{aligned} \tag{9}$$

The last approximation is justified since, even at 20 GHz, the previously assigned value of L_{FB} will contribute little as

$$\frac{\omega\, L_{FB}}{Z_0} = \frac{\omega\, C_{gs}}{G_m} = 0.081 \ll 1\,. \tag{10}$$

This means the impedance of L_{FB} is small when compared with the output loading impedance Z_0, and Z_{Miller} is now:

$$
\begin{aligned}
Z_{Miller} &= \frac{V_1}{j\,\omega\,C_{gd}\,(V_1 - V_2)} \\
&= \left(\frac{1}{j\,\omega\,C_{gd}} + \frac{L_{FB}\,G_m}{C_{gd}}\right)\frac{1}{1 + G_m\,Z_0} \\
&= \left(\frac{1}{j\,\omega\,C_{gs}} + \frac{L_{FB}\,G_m}{C_{gs}}\right)\frac{C_{gs}}{C_{gd}}\,\frac{1}{1 + G_m\,Z_0}\,.
\end{aligned}
\tag{11}
$$

This impedance expression is similar to that of looking into C_{gs} but has a much smaller value as

$$
\frac{C_{gs}}{C_{gd}}\,\frac{1}{1 + G_m\,Z_0} = \frac{1}{1 + 0.175 \cdot 50}\,\frac{113}{59} = \frac{1}{5}\,, \tag{12}
$$

which means the current flowing through C_{gd} is in phase but five times larger than the current on C_{gs}. The overall input impedance can now be re-arranged as

$$
Z_{in} = \left(\frac{1}{j\,\omega\,C_{gs}} + \frac{L_{FB}\,G_m}{C_{gs}}\right)\left[1 + \frac{C_{gd}}{C_{gs}}\,(1 + G_m\,Z_0)\right]^{-1}\,. \tag{13}
$$

By setting $\mathrm{Re}[Z_{in}] = Z_0$, there is

$$
\begin{aligned}
L_{FB} &= \frac{Z_0\,C_{gs}}{G_m}\left[1 + \frac{C_{gd}}{C_{gs}}\,(1 + G_m\,Z_0)\right] \\
&= 6\,\frac{Z_0\,C_{gs}}{G_m} \\
&= 194\ \mathrm{pH}\,,
\end{aligned}
\tag{14}
$$

i.e. with C_{gd} included in the transistor's small-signal model, the value of L_{FB} for a matched input needs to be increased six-fold. Still, as $\omega L_{FB} = 24\ \Omega$, the two approximations used in above hold:

$$
\begin{aligned}
\omega^2\,L_{FB}\,C_{gs} &\ll 1 \\
\frac{\omega\,L_{FB}}{Z_0} &\ll 1\,.
\end{aligned}
\tag{15}
$$

As for the so-far un-discussed R_{ds}, when its value changes from 1 to the measured 50 Ω, the feedback inductor L_{FB} needs to be adjusted again (Fig. 5). Neglecting the small current on C_{gd}, the current I_L on L_{FB} has the same magnitude but opposite polarity as that on the output loading impedance Z_0; therefore, from the conservation of current at either the source or the drain node, there is

$$
G_m\,V_c = I_L + \frac{j\,\omega\,L_{FB}\,I_L + Z_0\,I_L}{R_{ds}} \tag{16}
$$

or

$$I_L = \frac{R_{ds}}{R_{ds} + Z_0 + j\,\omega\,L_{FB}}\,G_m\,V_c \approx \frac{R_{ds}}{R_{ds} + Z_0}\,G_m\,V_c\,. \tag{17}$$

So

$$Z_{in} = \left(\frac{1}{j\,\omega C_{gs}} + \frac{L_{FB}\gamma G_m}{C_{gs}}\right)\left[1 + \frac{C_{gd}}{C_{gs}}\left(1 + \gamma G_m Z_0\right)\right]^{-1} \tag{18}$$

where $\gamma = R_{ds} = (R_{ds} + Z_0 + j\omega L_{FB})$ and can be treated as the degradation factor for transconductance G_m. In this case, the previously derived 194-pH L_{FB} can offer only 39.5 Ω for the transistor's input impedance. The value of L_{FB} needs to be increased to (194 • 50/39.5), or 246 pH to achieve the intended Re[Z_{in}]. Again, an input series inductor L_{series} can be brought in to eliminate at one frequency the capacitive part of Z_{in}.

B. Narrow-band input matching using capacitive feedback

If the transistor's output loading is a capacitor C_{FB} instead of the default characteristic impedance Z_0 (Fig. 6), then from the conservation of current at the drain node there is

$$j\,\omega\,C_{gd}\,(V_2 - V_1) + j\,\omega\,C_{FB} + G_m\,V_1 = 0 \tag{19}$$

or

$$V_2 = \frac{j\,\omega\,C_{gd} - G_m}{j\,\omega\,(C_{gd} + C_{FB})}\,V_1 \approx \frac{-G_m}{j\,\omega\,(C_{gd} + C_{FB})}\,V_1\,. \tag{20}$$

The last approximation holds because, even at 20 GHz, ωC_{gd} = 7.4 mS and is far smaller than G_m. The overall input admittance is then

$$\begin{aligned} Y_{in} &= j\,\omega\,C_{gs} + j\,\omega\,C_{gd}\left[1 + \frac{G_m}{j\,\omega\,(C_{gd} + C_{FB})}\right] \\ &= j\,\omega\,\left(C_{gs} + C_{gd}\right) + \frac{C_{gd}}{C_{gd} + G_{FB}}\,G_m\,. \end{aligned} \tag{21}$$

This is a shunt capacitor in parallel with a resistor. The value of C_{FB} for 50-Ω Re[Z_{in}] can be obtained by setting

$$\frac{1}{Z_0} = \frac{C_{gd}}{C_{gd} + G_{FB}}\,G_m \tag{22}$$

i.e.

$$C_{FB} = C_{gd}\,\left(G_m\,Z_0 - 1\right) = 7.75\,C_{gd}\,. \tag{23}$$

Intuitively, since the phase of the input current I_{in} is leading that of the input voltage V_c, this I_{in} can be decomposed into I and $j\Delta I$ where I is for the

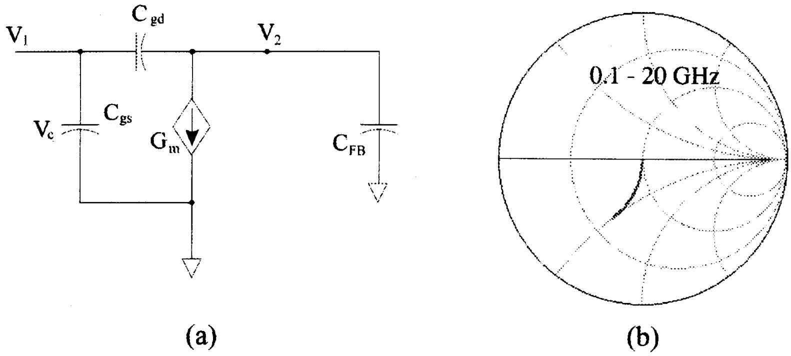

Fig. 6. Capacitive feedback using simplified transistor's small-signal model. (a) Schematic. In this transistor circuit, the drain resistor is assumed infinity. The ratio of the loading capacitor C_{FB} over the intrinsic capacitor C_{gd} determines the value of Re[Z_{in}]. (b) 0.1–20-GHz S_{11} on the Smith chart. This curve is similar to that of a resistive-feedback transistor circuit. An additional 49-pH L_{FB} (not shown here) at the source node will remove the capacitive part of Z_{in}.

equivalent resistor and $j\Delta I$ is for the capacitor. By adding a small inductor L_{FB} at the source node to offer a positive-phase $j\Delta V_c$, Z_{in} can be fine-tuned to Z_0 by forcing $V_c = I$ to be equal to $\Delta V_c = \Delta I$. Mathematically, the input voltage (with L_{FB} included) is

$$\begin{aligned} V_{in} &= V_c + j\,\omega\,L_{FB}\,(j\,\omega\,C_{gs}\,V_c + G_m\,V_c) \\ &= \left(1 - \omega^2\,L_{FB}\,C_{gs} + j\,\omega\,L_{FB}\,G_m\right)\,V_c \\ &\approx (1 + j\,\omega\,L_{FB}\,G_m)\,V_c\,. \end{aligned} \tag{24}$$

Since this L_{FB} has only minor impact on the drain side of the circuit, V_2–V_1 can be approximated as $V_2 - V_c$ and the total input current is

$$\begin{aligned} I_{in} &= I + j\,\Delta I \\ &= \left[\frac{C_{gd}}{C_{gd} + G_{FB}}\,G_m + j\,\omega\,(C_{gs} + C_{gd})\right]\,V_c \\ &= \frac{C_{gd}}{C_{gd} + G_{FB}}\,G_m\,\left[1 + j\,\omega\,(C_{gs} + C_{gd})\,\frac{C_{gd} + C_{FB}}{C_{gd}\,G_m}\right]\,V_c\,. \end{aligned} \tag{25}$$

By setting $C_{FB} = C_{gd}\,(G_m Z_0 - 1)$, or $V_c/I = Z_0$, there is

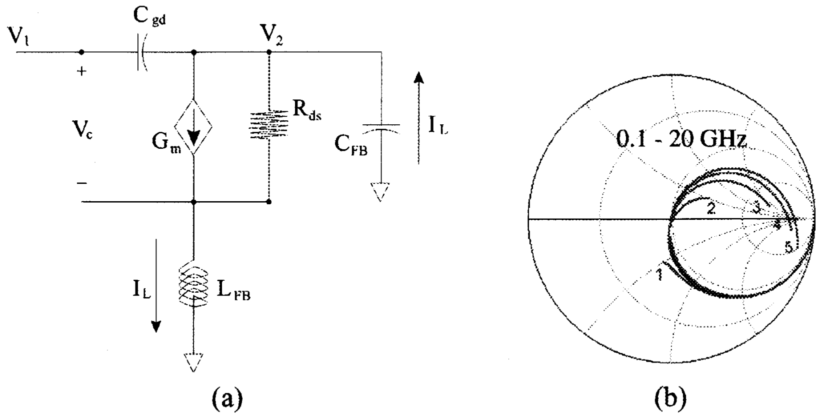

Fig. 7. Capacitive feedback. (a) Schematic. (b) With C_{FB} = 457 fF, curves 1 to 5 correspond to L_{FB} = 0, 50, 100, 150, 200 pH respectively. Here L_{FB} doesn't have much impact on the value of Re[Z_{in}].

$$Z_{in} = Z_0 \frac{1 + j\,\omega\, L_{FB}\, G_m}{1 + j\,\omega\, (C_{gs} + C_{gd})\, Z_0}. \tag{26}$$

Matched input impedance can be obtained by choosing L_{FB} as

$$L_{FB} = \frac{C_{gs} + C_{gd}}{G_m}\, Z_0\,. \tag{27}$$

For the TRW 200-um transistor, the value of this inductor is 49 pH. At 20 GHz, there is ωL_{FB} = 6.1 Ω and $\omega^2 L_{FB} C_{gs}$ = 0.045; the latter is far less than one, which justifies the approximation used in the above derivation. The impedance of C_{gs}, C_{gd}, and C_{FB} at 20 GHz are 70, 135, and 18.5 Ω respectively. On the Smith chart, C_{FB} will move the S_{11} curve to a fixed-acceptance contour and the inductance L_{FB} will suppress the curve down to a point. This picture is totally different from that of the conventional inductive feedback: Miller effect, or C_{gd}, is now highly desirable since it determines the value of Re[Z_{in}]. However, the above frequency-independent S_{11} comes from a transistor with infinite R_{ds}, which is unrealistic. To make this R_{ds} impact easier to comprehend, capacitor C_{gs} is omitted in the following analysis, so is the small current on the high impedance C_{gd} path (Fig. 7). Thus,

$$j\,\omega\, L_{FB}\, I_L + R_{ds}\, (I_L - G_m\, V_c) = V_2 \approx \frac{-I_L}{j\,\omega\, C_{FB}}\,. \tag{28}$$

By setting $Z_L = j\omega L_{FB}$ and $Z_C = 1 = 1/(j\omega C_{FB})$, it becomes

$$Z_L\, I_L + R_{ds}\,(I_L - G_m\, V_c) = -Z_C\, I_L\,. \tag{29}$$

Now step by step:

$$\begin{aligned}
I_L &= \frac{G_m\, R_{ds}}{R_{ds} + Z_C + Z_L}\, V_c \\
V_2 &= -Z_C\, I_L = -\frac{G_m\, R_{ds}\, Z_C}{R_{ds} + Z_C + Z_L}\, V_c \\
V_1 &= V_c + Z_L\, I_L = \left(1 + \frac{G_m\, R_{ds}\, Z_L}{R_{ds} + Z_C + Z_L}\right) V_c \\
\frac{V_1}{V_2} &= -\frac{R_{ds} + Z_C + Z_L + G_m\, R_{ds}\, Z_L}{G_m\, R_{ds}\, Z_C} \\
&= -\frac{1}{G_m\, Z_C}\left(1 + \frac{Z_C}{R_{ds}} + \frac{Z_L}{R_{ds}} + G_m\, Z_L\right) \\
Y_{Miller} &= j\,\omega\, C_{gd}\, \frac{V_1 - V_2}{V_1} = j\,\omega\, C_{gd} + \left(\frac{1}{j\,\omega\, C_{gd}}\, \frac{-V_1}{V_2}\right)^{-1}.
\end{aligned} \tag{30}$$

i.e.

$$\begin{aligned}
Y_{Miller} &= j\,\omega\, C_{gd} \\
&\quad + \left[\frac{C_{FB}}{G_m\, C_{gd}}\left[1 + \frac{1}{j\,\omega\, C_{FB}\, R_{ds}} + j\,\omega\, \frac{L_{FB}}{R_{ds}}\,(1 + G_m\, R_{ds})\right]\right]^{-1}.
\end{aligned} \tag{31}$$

This input admittance can be interpreted as a small capacitor C_{gd} in shunt with a *RLC* circuit where *R* is determined by C_{FB}, *C* comes from R_{ds}, and L_{FB} is used to remove the capacitance at one frequency:

$$\begin{aligned}
f_0 &= \frac{1}{2\,\pi}\, \frac{1}{\sqrt{L\,C}} \\
&= \frac{1}{2\,\pi}\, \frac{1}{\sqrt{L_{FB}\, C_{FB}\,(1 + G_m\, R_{ds})}} \\
&= \frac{0.051}{\sqrt{L_{FB}\, C_{FB}}}\,.
\end{aligned} \tag{32}$$

The 3 dB bandwidth Δf is

$$\begin{aligned}\Delta f &= f_0 R C \\ &= \left[\frac{1}{2\pi}\frac{1}{\sqrt{L_{FB}\,C_{FB}\,(1+G_m\,R_{ds})}}\right] C_{FB}\,R_{ds} \\ &= 2.55\sqrt{\frac{C_{FB}}{L_{FB}}}\,.\end{aligned} \tag{33}$$

The inclusion of R_{ds} causes the all-too-promising wide-band capacitive feedback being degraded back to a narrow-band one, which has matched input impedance at low frequency without any use of input i nductor L_{series}. For C_{FB} = 457 fF and L_{FB} = 200 pH, the calculated matching frequency is 0.051 times the square root of $L_{FB}C_{FB}$, or 5.3 GHz, and is agreeing with the simulated result. In this feedback mechanism, Re[Y_{in}] comes from the capacitive-loading Miller effect and is totally different from what happens in the inductive feedback.

C. Wide-band input matching using reactive feedback

As mentioned in our previous letter [7], by treating the capacitive feedback as a *RLC* resonator from the input perspective, its bandwidth can be broadened by introducing a lossy mechanism. A series output resistor R_{FB} can then be added to the original capacitive feedback circuit for this purpose (Fig. 8). Because this R_{FB} resistor can be from the input impedance of the second-stage transistor in the LNA circuit rather than a physical resistor, its noise impact is negligible. This noise consideration rules out the other possible R_{FB} location: namely, a physical resistor in series with the source inductor.

A more revealing interpretation for this new circuit configuration is that, since the capacitive feedback has a matched input impedance at low, or somehow medium, frequency, while the inductive feedback (without input L_{series}) is matched at a much higher frequency, a combination of these two circuit configurations should render a wide-band input match. Now with a $R_{FB}C_{FB}$ output loading and a L_{FB} on the source node of the transistor, this transistor circuit resembles a capacitive feedback circuit at low frequency since the impedance of C_{FB} is now much larger than R_{FB}; when the frequency increases, the capacitive feedback will be replaced gradually by the inductive feedback as $R_{FB}C_{FB}$ is now dominated by R_{FB}.

Since little if any insight can be gained from the rather tedious analytical expression for this wide-band Z_{in}, it is omitted here. However, it should be noted that this single transistor circuit has a good input match at even higher frequencies because no input inductor L_{series} is employed for the intended Re[Z_{in}]. Therefore, as frequency increases, S_{11} on the Smith chart converges to the matched point.

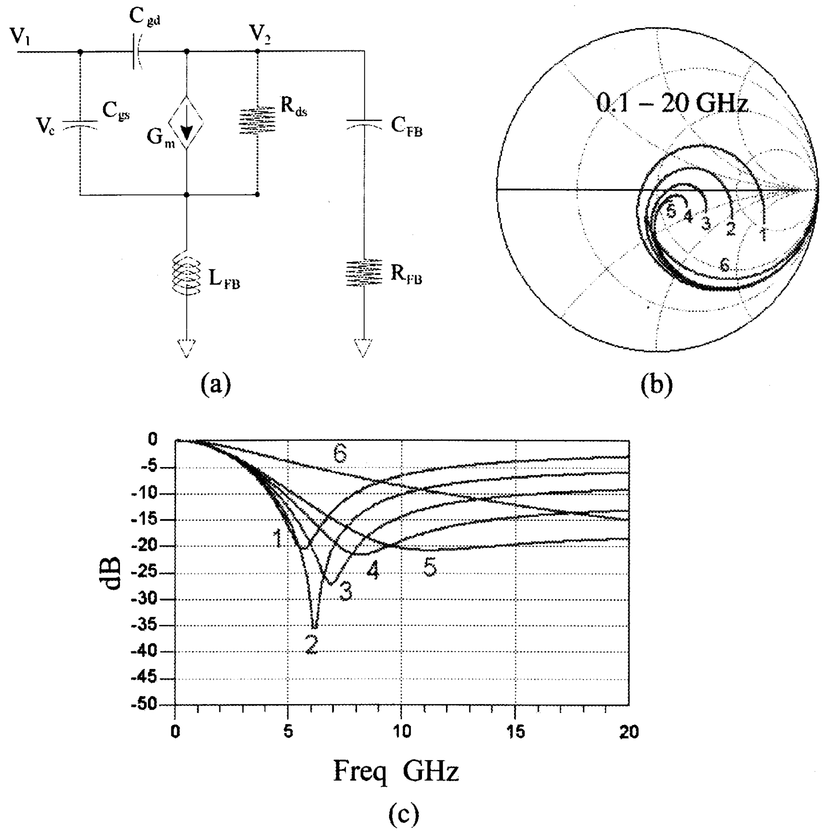

Fig. 8. Reactive feedback for wide-band input matching. (a) The combination of capacitive feedback and inductive feedback results in a wide-band input match. (b) The corresponding S_{11} of the TRW 200-um transistor in the reactive feedback configuration with C_{FB} = 457 fF, L_{FB} = 200 pH. Curves 1–5 correspond to R_{FB} = 0, 10, 20, 30, 40 Ω respectively, curve 6 is the inductive feedback with C_{FB} = 0 fF, R_{FB} = 50 Ω. Curves 2–5 can be interpreted as different combinations of curves 1 and 6. (c) S_{11} in dB. Curve 5 shows the intended wide-band response.

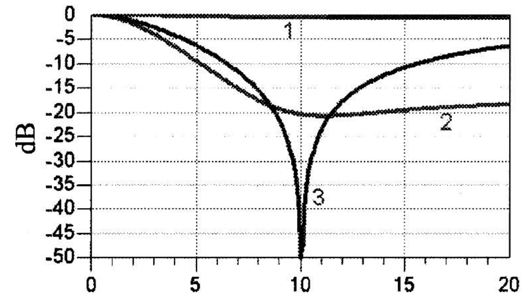

Freq GHz

(a)

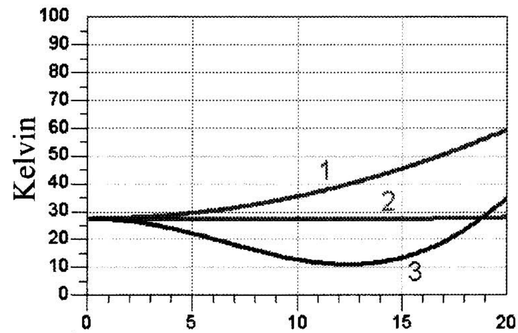

Freq GHz

(b)

Fig. 9. Simulated S_{11} and T_n of different transistor circuits. (a) S_{11} on the Smith chart. Curve 1 comes from the intrinsic TRW 200-um transistor. Curve 2 is from the reactive feedback circuit with 200-pH L_{FB} on the source node of the intrinsic transistor, 457-fF C_{FB} on the drain node and 40 Ω as output loading resistance. Curve 3 is from the conventional inductive feedback with 250-pH L_{FB} on the source node and 575-pH L_{series} at the input. (b) The corresponding noise temperature with T_{drain} set to 2100 Kelvin.

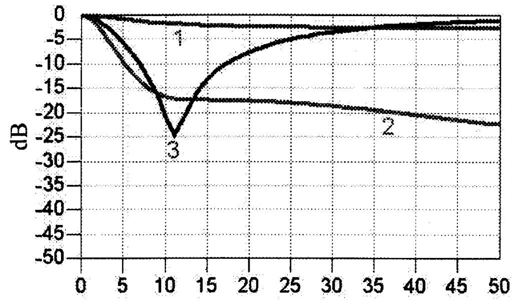

(a)

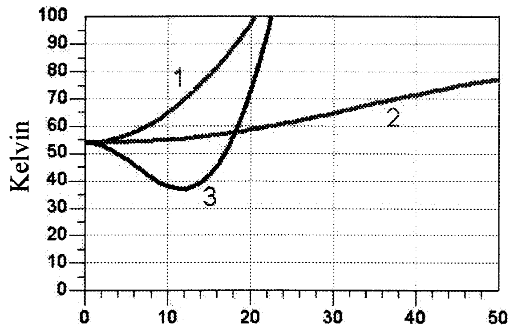

(b)

Fig. 10. Simulated S_{11} and T_n of different circuits using complete transistor model. (a) S_{11} on the Smith chart. Curve 1 is from the 15-element TRW 200-um transistor. Curve 2 is from the reactive feedback circuit with 200-pH L_{FB} on the source node of the transistor, 457-fF C_{FB} on the drain node and 40 Ω as output loading resistance. Curve 3 is from the conventional inductive feedback with 250-pH L_{FB} on the source and 575-pH L_{series} at the input. (b) The corresponding noise temperature with T_{drain} set to 2100 Kelvin.

D. Comparison of Noise Temperatures

As is clear from the simulated results (Figs. 9, 10), the revised feedback circuit does have a flat noise temperature vs. frequency while the inductive feedback with input inductor L_{series} has a locally optimized noise temperature. An in-depth understanding of the noise performance, which is beyond the reach of simulations, comes from mathematics. To derive the noise temperature o f the As is clear from the simulated results (Figs. 9, 10), the reactive feedback transistor circuit with source inductor L_{FB} on it, the relation between the drain noise current in and the resulting short-circuit output noise current i_{out} needs to be clarified (Fig. 11a). First, since the impedance of C_{gs} is much larger than the generator impedance ($1/Y_g$) at the frequency of interest, there is $v_c = -v_L$. By defining the impedance of L_{FB} as Z_L, the induced current on the G_m branch will have

$$\begin{aligned} v_c\, G_m &= -v_L\, G_m \\ &= -i_L\, (j\,\omega\, L_{FB})\, G_m \\ &= -i_L\, Z_L\, G_m\, . \end{aligned} \tag{34}$$

Based on the conservation of current at the transistor's source node while neglecting the small current flowing on C_{gs}, the relation between i_n and i_{out} is

$$\begin{aligned} i_L &= \frac{R_{ds}}{R_{ds} + Z_L}\, (-i_L\, Z_L\, G_m + i_n) \\ &\equiv \beta\, (-i_L\, Z_L\, G_m + i_n) \end{aligned} \tag{35}$$

i.e.

$$i_{out} = i_L = \frac{\beta}{1 + \beta\, G_m\, Z_L}\, i_n\, . \tag{36}$$

The next step is to find the relation between the output current i_{out} and the current i_g from the generator impedance, which can be carried out by linking the input current i_1 to voltage v_1 (Fig. 11b). The admittance Y_{IN} looking into the transistor circuit is derived via

$$\begin{aligned} v_1 &= \frac{1}{j\,\omega\, C_{gs}}\, i_1 + v_L \\ &= Z_c\, i_1 + Z_L\, i_L \\ &= Z_c\, i_1 + Z_L\, (G_m\, Z_c\, i_1)\, \frac{R_{ds}}{R_{ds} + Z_L} \\ &= Z_c\, i_1 + Z_L\, \beta\, G_m\, Z_c\, i_1 \\ &= \frac{1 + \beta\, Z_L\, G_m}{j\,\omega\, C_{gs}}\, i_1 \end{aligned} \tag{37}$$

i.e.

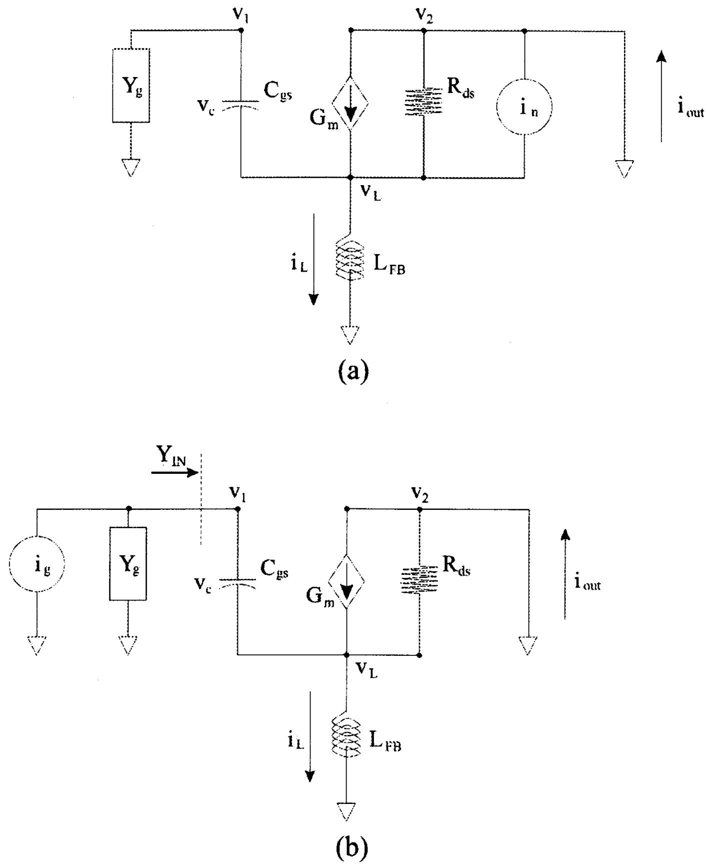

Fig. 11. Schematics for noise temperature derivation. (a) The noise current in from R_{ds} will bring upon current i_{out} at the short-circuit output. Here C_{gd} has been merged into Y_g to facilitate the derivation. (b) Noise current ig from the generator impedance will induce current i_{out} at the short-circuit output. Noise temperature of the inductive feedback circuit can be obtained by linking i_g to i_n, via i_{out}.

$$
\begin{aligned}
Y_{IN} &= \frac{i_1}{v_1} \\
&= \frac{1}{Z_c} \frac{1}{1 + \beta\, Z_L\, G_m} \\
&= \frac{j\,\omega\, C_{gs}}{1 + \beta\, j\,\omega\, L_{FB}\, G_m}.
\end{aligned}
\tag{38}
$$

Since R_{ds} is much larger than $|Z_L|$, this variable β can be treated as a real number. Input impedance Z_{IN} (= $1/Y_{IN}$) in the noise analysis is thus a capacitor in series with a resistor:

$$Z_{IN} = \frac{1}{Y_{IN}} = \frac{1}{j\,\omega\,C_{gs}} + \frac{L_{FB}\,\beta\,G_m}{C_{gs}}\,. \tag{39}$$

On the other hand, noise current i_g coming out of the generator admittance Y_g will bring upon an input noise current i_1 for this transistor circuit:

$$i_g = v_1\,(Y_g + Y_{IN}) \tag{40}$$

or

$$i_1 = v_1\,Y_{IN} = \frac{Y_{IN}}{Y_g + Y_{IN}}\,i_g\,. \tag{41}$$

Current i_1 will build a voltage on capacitor C_{gs}, which then induces a current on the drain side of the transistor. The output noise current i_{out} is therefore

$$i_{out} = i_L = \beta\,G_m\,Z_c\,i_1 = \beta\,G_m\,Z_c\,\frac{Y_{IN}}{Y_g + Y_{IN}}\,i_g \tag{42}$$

i.e.

$$i_g = \frac{1}{\beta\,G_m\,Z_c}\,\frac{Y_g + Y_{IN}}{Y_{IN}}\,i_{out}\,. \tag{43}$$

Thus

$$\begin{aligned} i_g &= \frac{1}{\beta\,G_m\,Z_c}\,\frac{Y_g + Y_{IN}}{Y_{IN}}\,\frac{\beta}{1 + \beta\,G_m\,Z_L}\,i_n \\ &= \frac{i_n}{G_m}\,(Y_g + Y_{IN})\,\frac{1}{Z_c}\,\frac{1}{Y_{IN}}\,\frac{1}{1 + \beta\,G_m\,Z_L} \\ &= \frac{i_n}{G_m}\,(Y_g + Y_{IN})\,\frac{1}{Z_c}\,[Z_c\,(1 + \beta\,Z_L\,G_m)]\,\frac{Z_c\,(1 + \beta\,Z_L\,G_m)}{1 + \beta\,G_m\,Z_L} \\ &= \frac{i_n}{G_m}\,(Y_g + Y_{IN}) \end{aligned} \tag{44}$$

Since in terms of unit bandwidth, there is, by definition,

$$\begin{aligned} T_{drain} &= \frac{\overline{|i_n^2|}}{4\,K_B/R_{drain}} \\ T_n &= \frac{\overline{|i_g^2|}}{4\,K_B\,G_g} \end{aligned} \tag{45}$$

where K_B is the Boltzmann's constant and the overhead of $\overline{|\ldots|}$ is the statistical averaging. Therefore,

$$\frac{T_n}{T_{drain}} = \frac{\overline{i_g^2}}{\overline{i_n^2}} \frac{1}{R_{drain}\, G_g} = \frac{|Y_g + Y_{in}|^2}{G_m^2} \frac{1}{R_{drain}\, G_g} \tag{46}$$

i.e.

$$\begin{aligned} T_n &= \frac{T_{drain}}{G_m^2} \frac{1}{R_{ds}\, G_g} \left|Y_g + Y_{IN}\right|^2 \\ &= \frac{T_{drain}}{G_m^2} \frac{1}{R_{ds}\, G_g} \left|G_g + j\left(X_g + \frac{\omega\, C_{gs}}{1 + j\,\omega\, L_{FB}\,\beta\, G_m} + \omega\, C_{gd}\right)\right|^2 \end{aligned} \tag{47}$$

where Y_{IN} is the admittance looking into the transistor circuit that has short-circuit output loading, and $\beta = R_{ds} = (R_{ds} + j\omega L_{FB})$. The inclusion of a source inductor L_{FB} indeed reduces the effective capacitance of C_{gs} and thus flattens the global noise temperature. Now it becomes clear why both the reactive and capacitive feedback circuits have low noise temperatures.

As for the conventional inductive feedback circuit where an inductor L_{series} is employed to remove the input Im[Y_{in}], the transistor's matched noise temperature can be obtained by merging L_{series} with the nominal 50-Ω generator impedance (Z_0). The revised generator admittance is:

$$\begin{aligned} Y_g &= \frac{1}{Z_0 + j\,\omega\, L_{series}} \\ &= \frac{Z_0}{Z_0^2 + \omega^2\, L_{series}^2} + j\,\frac{-\omega\, L_{series}}{Z_0^2 + \omega^2\, L_{series}^2} \\ &\equiv G_g + j\,X_g\,, \end{aligned} \tag{48}$$

and the corresponding noise temperature will be

$$T_n = \frac{T_{drain}}{G_m^2} \frac{1}{R_{ds}} \frac{Z_0^2 + \omega^2\, L_{series}^2}{Z_0} \left[A^2 + B^2\right] \tag{49}$$

with

$$\begin{aligned} A &= \frac{Z_0}{Z_0^2 + \omega^2\, L_{series}} \\ B &= \frac{-\omega\, L_{series}}{Z_0^2 + \omega^2\, L_{series}^2} + \frac{\omega\, C_{gs}}{1 + \beta\,\omega\, L_{FB}\, G_m} + \omega\, C_{gs} \end{aligned} \tag{50}$$

This L_{series} does bring upon a locally optimized T_n through the minus term in B's expression. At much higher frequency, the circuit's noise temperature will increase rapidly and is proportional to ω^2.

IV. Conclusion

In this paper, different circuit configurations used for wide-band amplifier design have been analyzed in detail. Through a full grasp of mathematics, the underlying physics of the most promising reactive-feedback mechanism, which is the combination of low-frequency-match capacitive feedback and high-frequency-match inductive feedback, is soundly explained. We believe this understanding of input matching mechanisms will facilitate the design of ultra-wide-band LNA's.

Acknowledgments

Author R. (Shu-I) Hu would like to thank S. Weinreb, M. Edgar, J. Kooi, D. Miller, N. Wadefalk, A. Shen, S. Lin, M. Yang and J. Zmuidzinas of the California Institute of Technology, Pasadena, CA; K.Y. Lo of the National Radio Astronomy Observatory (NRAO), Charlottesville, VA; M.P. Chen, P. Kosh and S.Y. Liu of the Institute of Astronomy and Astrophysics, Academia Sinica (ASIAA), Taipei, Taiwan for their support and encouragement.

References

[1] C.C. Chin, *et al*, "A low-noise 100 GHz sideband separating receiver," *Intl. J. IR & MM Waves,* vol. 24, pp. 569–600, April 2004.

[2] R. Rice, M. Sumner, J. Zmuidzinas, R. Hu, H.G. Leduc, A.I. Harris, D. Miller, "SIS mixer design for a broadband millimeter spectrometer suitable for rapid line surveys and redshift determinations," *Proc. SPIE,* vol. 4855, pp. 301–311, Feb. 2003.

[3] J. Yang, S. Huang, M. Ohishi, K. Miyazawa, R. Henneberger, "A 492 GHz submillimeterwave receiver," *Intl. J. IR & MM Waves,* vol. 22, pp. 217–223, Feb. 2001.

[4] I.L. Fernandiz, J.D. Gallego, C. Diez, A. Barcia, J.M. Pintado, "Wide-band ultra low noise cryogenic InP IF amplifiers for the Herschel mission radiometers," *Proc. SPIE,* vol. 4855, pp. 489–500, Feb. 2003.

[5] N. Wadefalk, *et al.*, "Cryogenic Wide-Band Ultra-Low-Noise IF Amplifiers Operating at Ultra-Low DC Power," *IEEE Trans. Microwave Theory Tech.,* vol. 51, pp. 1705–1711, June 2003.

[6] S. Weinreb, D. L. Fenstermacher, R. W. Harris, "Ultra-low-noise 1.2- to 1.7-GHz cooled GaAsFET amplifiers," *IEEE Trans. Microwave Theory Tech.,* vol. 82, pp. 849–853, June 1982.

[7] R. Hu, "An 8–20 GHz LNA design and the analysis of its input matching mechanism," *IEEE Microwave and Wireless Components Letter,* vol. 14, pp.

528–530, Nov. 2004.

[8] T.K. Nguyen, C.H. Kim, G.J. Ihm, M.S. Yang, S.G. Lee, "CM OS low-noise amplifier design optimization techniques," *IEEE Trans. Microwave Theory Tech.,* vol. 52, pp. 1433-1442, May 2004.

[9] D. Lu, D. Rutledge, M. Kovacevic, J. Hacker, "A 24-GHz patch array with a power amplifier/low-noise amplifier MMIC," *Intl J. IR & M Waves,* vol. 23, pp. 693–704, May 2002.

[10] G. Gonzalez, "Microwave transistor amplifier: analysis and design," *Prentice-Hall Inc.* ISBN 0135816467, 1984.

[11] R. Hu, S. Weinreb, "A novel wide-band noise-parameter measurement method and its cryogenic application," *IEEE Trans. Microwave Theory Tech.,* vol. 52, pp. 1498–1507, May 2004.

[12] R. A. Minasian, "Simplified GaAs MESFET model to 10 GHz," *Electronic letter,* pp. 549–551, Sep. 1977.

[13] M. Berroth, R. Bosch, "Broad-band determination of the FET small-signal equivalent circuit," *IEEE Trans. Microwave Theory Tech.,* vol. 38, pp. 891–895, July 1990.

[14] G. Dambrine, A. Cappy, F. Heliodore, E. Playez, "A new method for determining the FET small-signal equivalent circuit," *IEEE Trans. Microwave Theory Tech.,* vol. 36, pp. 1151–1159, July 1988.

[15] A. Eskandarian, S. Weinreb, "A note on experimental determination of small-signal equivalent circuit of millimeter-wave FETs," *IEEE Trans. Microwave Theory Tech.,* vol. 41, pp. 159–162, Jan. 1993.

[16] M. W. Pospieszalski, "Modeling of noise parameters of MESFET's and MODFET's and their frequency and temperature dependence," *IEEE Trans. Microwave Theory Tech.,* vol. 37, pp. 1340–1350, Sep. 1989.

[17] F. Danneville, H. Happy, G. Dambrine, J. M. Belquin, A. Cappy, "Microscopic noise modeling and macroscopic noise modeling: How good a connection," *IEEE Trans. Microwave Theory Tech.,* vol. 42, pp. 779–786, May 1994.

[18] J. H. Han, K. Lee, "A new extraction method for noise sources and correlation coefficient in MESFET," *IEEE Trans. Microwave Theory Tech.,* vol. 44, pp. 487–490, Mar. 1996.

[19] K. B. Niclas, W. T. Wilser, R. B. Gold, W. R. Hitchens, "The matched feedback amplifier: ultra-band microwave amplification with GaAs

MESFET's," *IEEE Trans. Microwave Theory Tech.,* vol. 28, pp. 285–294, April 1980.